






# Microcontroller Execution, Random Number Generation and Chaos Annihilation in Piecewise Quadratic Map

Lucienne Makouo <sup>\*,1</sup>, Jules Metsebo <sup>α,2</sup>, Cyrille Ainamon <sup>β,3</sup>, Oumate Alhadji Abba <sup>§,4</sup> and André Chéagé Chamgoué <sup>\*\*,5</sup>

<sup>\*</sup>Department of Civil Engineering and Architecture, National Higher Polytechnic Institute, University of Bamenda, P.O. Box 39, Bamenda, Cameroon, <sup>α</sup>Department of Hydraulics and Water Management, National Advanced School of Engineering, University of Maroua, P.O. Box 46 Maroua, Cameroon, <sup>β</sup>Institut de Mathématiques et de Sciences Physiques, Université d'Abomey-Calavi, BP 613, Porto Novo, Benin, <sup>§</sup>Department of Physics, Faculty of Science, University of Maroua, P.O. Box 814, Maroua, Cameroon, <sup>\*\*</sup>Department of Petroleum and Gas Engineering, School of Geology and Mining Engineering, University of Ngaoundere, P.O. BOX 115, Meiganga, Cameroon.

**ABSTRACT** This paper presents the study of microcontroller execution, pseudo random number generator (PRNG) and chaos annihilation in a piecewise quadratic map (PQM). PQM is generated by replacing the cubic nonlinearity of cubic map by absolute nonlinearity. Bistable outphase and monostable chaotic characteristics and bistable outphase periodic oscillations are encountered in PQM during numerical simulations. The microcontroller execution of PQM is realized to validate the numerical results encountered in PQM. The PRNG derived from the PQM is made and the NIST 800-22 statistical test validated it. Finally, analytical calculations and numerical simulations show the effectiveness of chaos annihilation in PQM using feedback controller.

## KEYWORDS

Chaotic maps  
Microcontroller execution  
RNG  
Chaos annihilation

## INTRODUCTION

Discrete chaotic maps are usually iterated mathematical function that display chaotic behavior. They have aroused the interest of physicists, engineers, mathematicians, chemists, population biologists, and many others (Bergé *et al.* 1987; Moon 1987; Zeng *et al.* 1990). They have a common characteristic, namely nonlinearity and their behavior depends on certain controllable quantities. Nonlinearity is a characteristic of a system or function where the output is not a simple multiple of the input (Abdullaev *et al.* 2002). The nonlinearity can be classified as smooth and nonsmooth functions (Rapcsák 2008; Aguirre 2014). Piecewise nonlinearities belong to a class of nonsmooth functions used to describe dynamical systems having intermittent contact, as mechanical systems with moving parts (Zhang *et al.* 2022; Chávez *et al.* 2016).

The most popular chaotic map is the logistic map which first appeared during the study of population in ecology (May 1987). It is nowadays used to describe many natural processes and has been the subject of numerous studies (Chen *et al.* 2021; Das *et al.* 2010; Dua *et al.* 2024). Logistic chaotic map has smooth function as

nonlinearity which is quadratic function. Cubic map belongs to the same universality class as the logistics map (Ambika and Joseph 1992). Cubic chaotic map has smooth function as nonlinearity which is cubic function. Since the cubic map has been proposed in (Rogers and Whitley 1983; Zeng 1985) which demonstrated the existence of a period doubling route to chaos. It has been subjected to detailed studies (Steeb *et al.* 1997; Wang *et al.* 2021). A piecewise cubic map (PCM) described by piecewise-nonlinear function with two parameters has been proposed in (Udwadia and Guttalu 1989). The authors of (Udwadia and Guttalu 1989) investigated analytically and numerically the PCM to find the route to chaos. The motivation for this research paper stems from the Lozi chaotic map (Lozi 2023) where Lozi replaced the quadratic term in the Henon chaotic map (García-Martínez and Campos-Cantón 2015) by an absolute value function.

Since 1978, Lozi chaotic map has been extremely studied and continues to be. Hundreds of publications have investigated its particular characteristics and applied its properties in many fields via algorithms (Lozi 2023). Inspired by Lozi chaotic map, this paper designs a PQM generated by replacing the cubic nonlinearity of cubic map by absolute nonlinearity. It studies the microcontroller execution, PRNG and chaos annihilation in designed PQM. The tri-modal map derived from the logistic map which belongs to the family of chaotic PQM has been proposed in (García-Martínez and Campos-Cantón 2015). The authors of (García-Martínez and Campos-Cantón 2015) has been demonstrated that it was pos-

**Manuscript received:** 4 November 2025,

**Revised:** 16 December 2025,

**Accepted:** 30 December 2025.

<sup>1</sup>makouol@yahoo.fr (Corresponding author).

<sup>2</sup>jmetsebo@gmail.com

<sup>3</sup>ainamoncyrille@yahoo.fr

<sup>4</sup>oumat\_oaa@yahoo.fr

<sup>5</sup>acchamgoue@gmail.com

sible to have PRNG based on chaotic tri-modal map. The one-dimensional piecewise map derived from the logistic map has been proposed in (Cassal-Quiroga *et al.* 2022).

The authors of (Cassal-Quiroga *et al.* 2022) has been demonstrated analytically and numerically that the proposed piecewise map was able to display bistability phenomenon, coexisting and chaotic attractors. This research paper demonstrated: (1) numerically and experimentally bistable outphase and monostable chaotic characteristics and bistable outphase periodic oscillations in PQM and; (2) the possibility to have PRNG based on chaotic PQM and (3) the chaos annihilation in PQM using a feedback controller. This paper is organized in the following manner: The second section deals with the microcontroller execution of the designed PQM. The PRNG based on designed PQM is studied in the third section. The fourth section deals with the chaos annihilation in the designed PQM. The fifth section concludes this paper.

### MICROCONTROLLER VALIDATION OF PQM

The PQM is designed by replacing the term  $x_n^3$  in the cubic map (Wang *et al.* 2021) by the term  $x_n |x_n|$ . It is described by:

$$x_{n+1} = \beta x_n - x_n |x_n| \quad (1)$$

where  $x_n$  and  $x_{n+1}$  respectively represent the  $n^{th}$  and  $(n + 1)^{th}$  states with  $n$  being a natural number and  $\beta$  is positive constant. The PQM described by map (1) can be also written as follows:

$$x_{n+1} = \begin{cases} \beta x_n + x_n^2, & x_n < 0, \\ \beta x_n - x_n^2, & x_n \geq 0. \end{cases} \quad (2)$$

The dynamical characteristics encountered in PQM are depicted in Fig. 1.

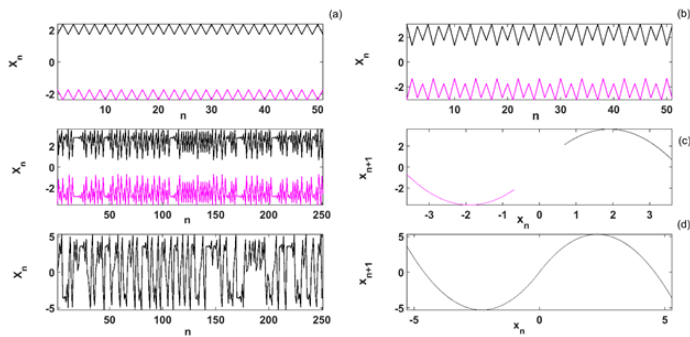


**Figure 1** Dynamical characteristics of PQM for specific values of  $\beta$ : (a)  $\beta = 3.1$ , (b)  $\beta = 3.6$ , (c)  $\beta = 3.8$  and (d)  $\beta = 4.6$ . The plots in black are generated using the initial states:  $x_0 = 0.1$  whereas the plots in magenta are generated with the initial states  $x_0 = -0.1$ .

The PQM displays bistable outphase period-1-oscillations in Fig. 1 (a), bistable outphase period-2-oscillations in Fig. 1 (b), bistable outphase chaotic characteristics in Fig. 1 (c) and monostable chaotic characteristics in Fig. 1 (d). The experimental set-up diagram of PQM microcontroller execution is elaborated in Figure 2.

The practical set-up of Fig. 2 is constituted of a digital platform based on the STM32F4xx series board, incorporating an ARM Cortex M4-based microcontroller for signal processing and a RIGOL DHO804 digital oscilloscope for visualization of phase portraits

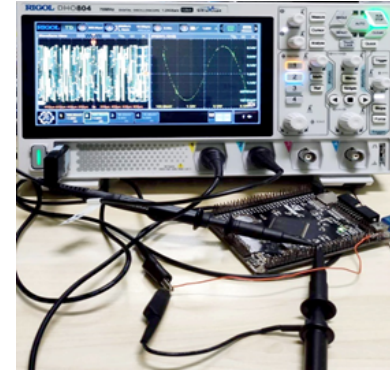


**Figure 2** Arrangement of the equipment for the microcontroller execution of PQM.

and time-series data. The Arduino code is then written, compiled, and the resulting binary file by the device are converted to analog using the integrated digital-to-analog converter of the STM32F4xx board. Figs 3 and 4 illustrate time-series and function given by the PQM from the microcontroller execution, showing different qualitative behavior of PQM.

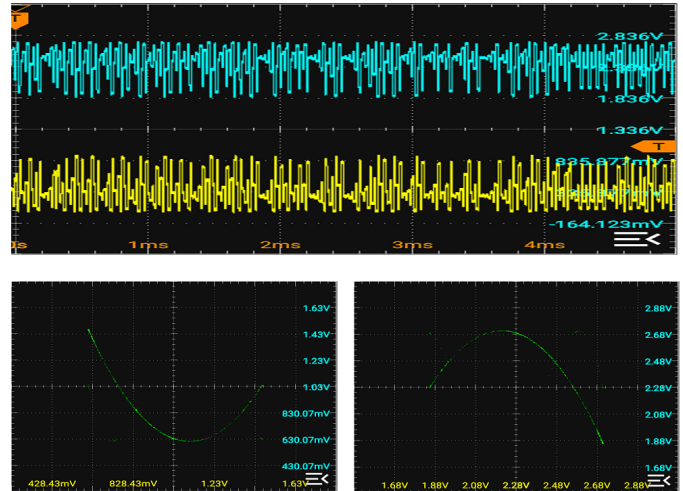


**Figure 3** Bistable outphase chaotic characteristics via the microcontroller execution of PQM.

Figures 3 and 4 display bistable and monostable chaotic characteristics, respectively gotten from the microcontroller execution of PQM described by map (1). The microcontroller results of Figs 3 and 4 validate the numerical results of Figs 1 (c) and 1 (d).

### RANDOM NUMBER GENERATOR BASED ON PQM

In this following, the design process of a PQM-based PRNGs is presented and the resulting module is tested following the widely used NIST 800-22 package. It is a battery of up to fifteen statistical tests to evaluate the random nature of a Boolean sequence for cryptography purpose. The NIST 800-22 tests analyze the properties of a long binary array by checking the presence or the absence of specific patterns. All the tests must be successful without exceptions to validate a given binary sequence as random. The computed values of the state variable  $x_n$  are scaled up and converted on sixteen bits.

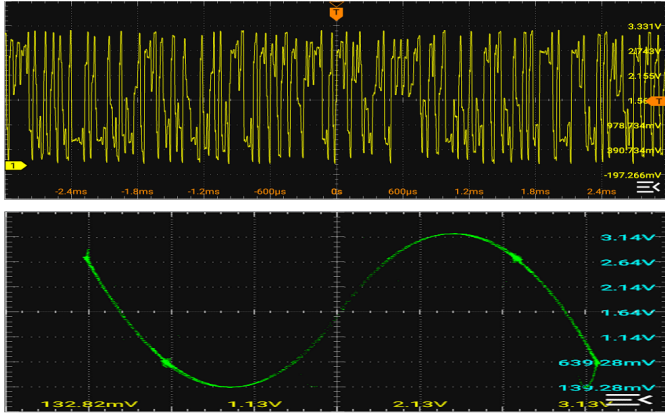


**Figure 4** Monostable chaotic characteristics via the microcontroller execution of PQM.

Subsequently, the eight least significant binary digits  $B$  are considered and re-ordered to obtain an 8-bit output key  $K$ . The process is repeated until the required data length is attained. The collected binary sequence is tested and validated with the NIST test suite. If a single test failed, scaling factor  $k_p$ , map parameter  $\beta$ , initial condition  $x(0)$  and the arrangement of computed output bits are fine-tuned to achieve better results. Upon successful, the generated sequences' randomness is validated, confirming the PRNG design's success. The operation of the designed PQM-PRNG is described in the pseudocode of Algorithm 1.

**Algorithm 1** Pseudocode of the Designed PQM-PRNG

- 1: Initialize parameters:  $k_p = 2^{32}$ ,  $\beta = 4.6$ ,  $result = 1.0$
- 2: Set initial condition:  $x = 0.1$
- 3:  $n\_bits \leftarrow 0$
- 4: **while**  $n\_bits < 1,000,000$  **do**
- 5:    $x \leftarrow \beta \cdot x - x \cdot |x|$
- 6:    $result \leftarrow k_p \cdot x$
- 7:    $X \leftarrow float\_to\_binary(result, 16)$
- 8:    $B \leftarrow lsb(X, 8)$
- 9:    $K \leftarrow reorder(B)$
- 10:   Append  $K$  to file `binarysequence.bin`
- 11:    $n\_bits \leftarrow n\_bits + 8$

In Algorithm 1, the functions `float_to_binary`, `lsb` and `reorder` are used to respectively convert a real number into a 16-bit binary sequence, extract the 8 least significant bit of a 16-bit sequence and rearrange the element of an 8-bit binary number. Several option of re-ordering are tested and the following re-arrangement:  $K(1) \leftarrow B(5)$ ;  $K(2) \leftarrow B(3)$ ;  $K(3) \leftarrow B(7)$ ;  $K(4) \leftarrow B(1)$ ;  $K(5) \leftarrow B(8)$ ;  $K(6) \leftarrow B(4)$ ;  $K(7) \leftarrow B(6)$ ;  $K(8) \leftarrow B(2)$ ; ensures good results for the chosen set of parameters. Fig. 5 illustrates the design flowchart of the PQM-based PRNG.

Among the numerous possible combination, a set of parameters allowing the designed PRNG to validate all NIST 800-22 test is:  $k_p = 2^{32}$ ,  $x_n(0) = 0.1$ ,  $\beta = 4.6$  and the output re-arranged as  $\{Key\} = \{X_1 X_2 X_3 X_4 X_5 X_6 X_7 X_8\}$ . The randomness is determined for each test by assessing the p-value, with the significance threshold set at 0.01 suggesting that the data's randomness is evaluated with a 99 confidence. A 1Mbit of data file containing the binary sequence generated from PQM-based PRNG is loaded and tested.

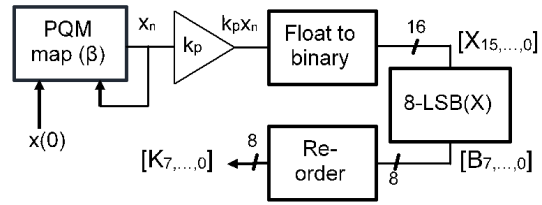


**Figure 5** Functional block diagram of the proposed PQM-based PRNG.

The NIST evaluation results are given in Table 1.

**Table 1** NIST Evaluation Results

Test Name	P-value	Result
Frequency	0.4703	Passed
Block Frequency	0.4094	Passed
Runs	0.9977	Passed
Longest Run	0.9145	Passed
Matrix Rank	0.1205	Passed
Spectral	0.7342	Passed
Non-overlapping Template Matching	0.5682	Passed
Overlapping Template Matching	0.2358	Passed
Universal	0.7965	Passed
Linear Complexity	0.0422	Passed
Serial	0.8595	Passed
Approximate Entropy	0.9048	Passed
Cumulative Sums (Cusum)	0.8110	Passed
Random Excursions	0.3607	Passed
Random Excursions Variant	0.2824	Passed

The  $p$ -values of the  $x_n$  signal pass successful the fifteen statistical evaluations of NIST 800-22 as shown in Table 1. The random signal generated from chaotic PQM can be used in applications such as secure communication schemes and other chaos-based applications.

**CHAOS ANNIHILATION IN PQM**

Section 4 is devoted to the context of chaos annihilation which is different to the context of generating pseudorandom numbers. A feedback controller (Wang and Wang 2008) is used to annihilate chaos in PQM in this section. The controlled PQM can be described by:

$$x_{n+1} = \beta x_n - x_n |x_n| + (\hat{x} - \kappa x_n) \quad (3)$$

where  $\kappa$  is the feedback coefficient and  $\hat{x}$  stands for the fixed points of map (1):  $\hat{x} = 0$  and  $\hat{x} = \pm(\beta - 1)$ . By choosing to stabilize PQM described by the map (3) at using the feedback controller, the Jacobian matrix of map (3) at  $\hat{x} = 0$  is:

$$J_{(\hat{x}=0)} = (\beta x - |x| - x \text{sign}(x) - \kappa)_{(\hat{x}=0)} = \beta - \kappa \quad (4)$$

If  $|\beta - \kappa| < 1$ , i.e.  $\beta - 1 < \kappa < \beta + 1$ , map (3) will be stabilized at a fixed point  $\hat{x} = 0$ . The bifurcation diagram of map (3) and Lyapunov exponent (LE) with respect to the feedback coefficient  $\kappa$  in Fig. 6.

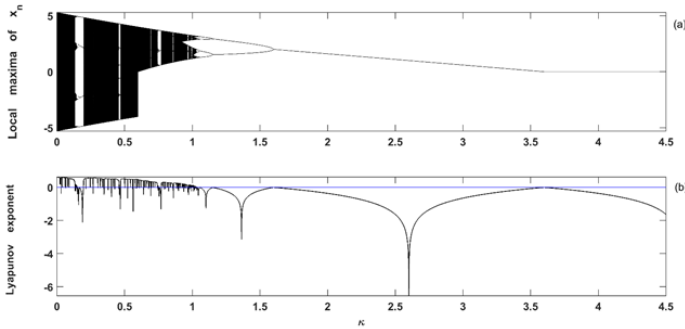


**Figure 6** Local maxima of  $x_n$  (a) and LE (b) versus the feedback coefficient  $\kappa$  for  $\beta = 4.6$ ,  $\hat{x} = 0$  and the initial states:  $x_0 = 0.1$ .

The controlled PQM described in map (3) exhibits reverse period doubling to chaotic region interspersed by periodic windows, limit cycle, Hopf bifurcation  $\kappa \approx 3.6$  and fixed point as illustrated in Fig. 6 (a). The dynamical characteristics encountered in Fig. 6 (a) are corroborated by its corresponding LE in Fig. 6 (b). Fig. 6 reveals that the feedback controller can annihilate the chaos encountered in PQM. From Fig. 6 (a), one can see that for  $\kappa = \beta - 1 = 3.6$  map (3) has a Hopf bifurcation, for  $\kappa > \beta + 1 = 5.6$  map (3) is divergent and for  $3.6 < \kappa < 5.6$  is stabilized at  $\hat{x} = 0$ . Therefore, the simulations results are consistent with the analytical calculations. Furthermore, the effects of chaos annihilations in PQM using the feedback controller are more illustrated in the time series as shown in Fig. 7.

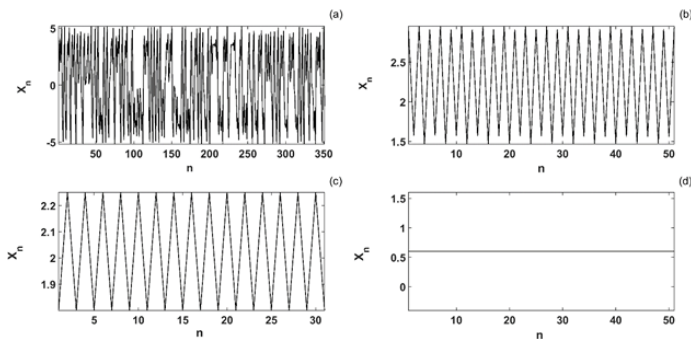


**Figure 7** Times series of  $x_n$  for specific values of  $\kappa$ : (a)  $\kappa = .005$ , (b)  $\kappa = 1.15$ , (c)  $\kappa = 1.55$  and (d)  $\kappa = 3.5$ . The others parameters are  $\beta = 4.6$ ,  $\hat{x} = 0$  and the initial states:  $x_0 = 0.1$ .

The amplitude of  $x_n$  exhibits chaos in Fig. 7 (a), period-2-oscillations in Fig. 7 (b), limit cycle in Fig. 7 (c) and fixed point in Fig. 7 (d).

## CONCLUSION

This paper explored the microcontroller execution, pseudo random number generator (PRNG) and chaos annihilation in a piecewise quadratic map (PQM). PQM was designed by replacing the cubic term of cubic map by absolute nonlinearity. During numerical simulations, PQM revealed the monostable and bistable outphase chaotic characteristics and bistable outphase periodic characteristics. The numerical results encountered in PQM was confirmed through microcontroller execution and the two results were found to be in perfect agreement. The randomness of the PRNG was extensively tested using the NIST 800-22 test suite, confirming the suitability of PQM-based PRNG for applications such as secure communication schemes and other chaos-based applications. It was demonstrated that the analytical calculations and numerical simulations confirmed the effectiveness of chaos annihilation in PQM using the feedback controller.

## Ethical standard

The authors have no relevant financial or non-financial interests to disclose.

## Availability of data and material

Not applicable.

## Conflicts of interest

The authors declare that there is no conflict of interest regarding the publication of this paper.

## LITERATURE CITED

- Abdullaev, F., O. Bang, and M. P. Sørensen, 2002 *Nonlinearity and Disorder: Theory and Applications*, volume 45. Springer Science & Business Media.
- Aguirre, L. A., 2014 Identification of smooth nonlinear dynamical systems with non-smooth steady-state features. *Automatica* **50**: 1160–1166.
- Ambika, G. and K. B. Joseph, 1992 Deterministic chaos—the period doubling and intermittency routes. *Pramana* **39**: 193–252.
- Bergé, P., Y. Pomeau, and C. Vidal, 1987 *Order within chaos* new york.
- Cassal-Quiroga, B., H. Gilardi-Velázquez, and E. Campos-Cantón, 2022 Multistability analysis of a piecewise map via bifurcations. *International Journal of Bifurcation and Chaos* **32**: 2250241.
- Chávez, J. P., Y. Liu, E. Pavlovskaja, and M. Wiercigroch, 2016 Path-following analysis of the dynamical response of a piecewise-linear capsule system. *Communications in Nonlinear Science and Numerical Simulation* **37**: 102–114.
- Chen, S., S. Feng, W. Fu, and Y. Zhang, 2021 Logistic map: Stability and entrance to chaos. In *Journal of Physics: Conference Series*, volume 2014, p. 012009, IOP Publishing.
- Das, N., R. Sharmah, and N. Dutta, 2010 Period doubling bifurcation and associated universal properties in the verhulst population model. *International J. of Math. Sci. & Engg. Appls* **4**: 1–14.
- Dua, M., R. Bhogal, S. Dua, and N. Chakravarty, 2024 Satellite image encryption using amalgamation of randomized three chaotic maps and dna encoding. *Physica Scripta* **100**: 015241.
- García-Martínez, M. and E. Campos-Cantón, 2015 Pseudo-random bit generator based on multi-modal maps. *Nonlinear Dynamics* **82**: 2119–2131.

- Lozi, R., 2023 Survey of recent applications of the chaotic lozi map. *Algorithms* **16**: 491–553.
- May, R. M., 1987 Chaos and the dynamics of biological populations. *Proceedings of the Royal Society of London. A. Mathematical and Physical Sciences* **413**: 27–44.
- Moon, F. C., 1987 *Chaotic vibrations: An introduction for applied scientists and engineers* new york.
- Rapcsák, T., 2008 Smooth nonlinear nonconvex optimization. In *Encyclopedia of Optimization*, pp. 3622–3625, Springer.
- Rogers, T. D. and D. C. Whitley, 1983 Chaos in the cubic mapping. *Mathematical Modelling* **4**: 9–25.
- Steeb, W., F. Solms, T. K. Shi, and R. Stoop, 1997 Cubic map, complexity and ljustapunov exponent. *Physica Scripta* **55**: 520.
- Udwadia, F. E. and R. S. Guttalu, 1989 Chaotic dynamics of a piecewise cubic map. *Physical Review A* **40**: 4032.
- Wang, C., Y. Di, J. Tang, J. Shuai, Y. Zhang, *et al.*, 2021 The dynamic analysis of a novel reconfigurable cubic chaotic map and its application in finite field. *Symmetry* **13**: 1420.
- Wang, X. and M. Wang, 2008 Chaotic control of logistic map. *Modern Physics Letters B* **22**: 1941–1949.
- Zeng, W.-z., 1985 A recursion formula for the number of stable orbits in the cubic map. *Chin. Phys. Lett.* **2**: 429–431.
- Zeng, X., R. Pielke, and R. Eykholt, 1990 Chaos in daisyworld. *Tellus B* **42**: 309–318.
- Zhang, Z., J. Páez Chávez, J. Sieber, and Y. Liu, 2022 Controlling grazing-induced multistability in a piecewise-smooth impacting system via the time-delayed feedback control. *Nonlinear Dynamics* **107**: 1595–1610.

**How to cite this article:** Makouo, L., Metsebo, J., Ainamon, C., Abba, O. A., and Chamgoué, A. C. Microcontroller Execution, Random Number Generation and Chaos Annihilation in Piecewise Quadratic Map. *ADBA Computer Science*, 3(1), 13-17, 2026.

**Licensing Policy:** The published articles in ACS are licensed under a [Creative Commons Attribution-NonCommercial 4.0 International License](https://creativecommons.org/licenses/by-nc/4.0/).

